Mineral Identification of Iron Ore Deposits in Menggamat, South Aceh through Mineralogical Analysis

Mislina [a,1], Dian Maulina [a,2], Balkhaya[b,3,*], Afdhal [a,4], Hasbaini[a,5]

[a] *Study Program of Industrial Engineering, Polytechnic of South Aceh, Merdeka Street, Beach Reclamation Area, Tapaktuan City, 23751, Indonesia*
[b] *Program Study of Mechanical Engineering, Polytechnic of South Aceh, Merdeka Street, Beach Reclamation Area,Tapaktuan city, 23751, Indonesi*
[1]*ummialif123@gmail.com;* [2] *dianmaulina312@gmail.com;* [3] *balkhaya@gmail.com*;* [4]*afdhal.m.isa@gmail.com,;* [5]*hasbainibean@gmail.com*
*Corresponding author

ARTICLE INFO

Article history:
Published
January 9, 2026

Keywords:
Iron ore mineralization;
Ore mineralogy;
Mineragraphic analysis;
Replacement texture;
Kluet Tengah

ABSTRACT

Iron ore mineralization in the Menggamat area, Kluet Tengah District, South Aceh Regency, has been exploited by local communities; however, detailed mineralogical studies remain limited. This study aims to identify the main ore minerals, associated minerals, microscopic textures, and paragenetic sequence of iron ore deposits using an integrated mineralogical approach. Field investigations were conducted in Simpang Dua and Simpang Tiga villages, where 31 rock samples were collected through channel sampling, chip sampling, and grab sampling methods. Macroscopic observations were followed by petrographic and mineragraphic analyses using reflected and transmitted light microscopy. The results indicate that magnetite and hematite are the dominant iron ore minerals, accompanied by sulfide minerals such as pyrite and chalcopyrite. Gangue and alteration minerals include quartz, garnet, and carbonate minerals. Mineragraphic observations reveal abundant replacement, crosscutting, intergrowth, and inclusion textures, indicating a multistage mineralization process. Magnetite represents the earliest mineral phase, subsequently replaced by hematite through oxidative alteration, followed by metasomatic replacement by garnet and late-stage quartz veining. These mineralogical characteristics and textural relationships suggest that the iron ore deposits in the study area are genetically related to skarn-type mineralization associated with hydrothermal and metasomatic processes. The results provide essential baseline data for sustainable mineral resource management and preliminary environmental assessment in South Aceh.

I. Introduction

South Aceh is one of the regions in Aceh Province that possesses significant potential for both metallic and non-metallic mineral resources. Non-metallic minerals, such as marble, have been reported at several locations, while metallic mineral resources particularly iron ore, copper, and gold are distributed across multiple districts but remain insufficiently supported by comprehensive scientific studies [1], [4]. The exploitation of mineral resources without reliable geological and mineralogical data may lead to environmental and social problems, especially in areas that have experienced mining activities.

One area indicating the presence of iron ore deposits is Kluet Tengah District, South Aceh Regency. This district comprises several villages, including Simpang Tiga, where iron ore mining activities have been conducted by local communities and certain parties. However, scientific identification of the main ore minerals and associated minerals within these iron ore deposits remains very limited. Local communities generally recognize the extracted material only as “iron ore,” without understanding the presence of other minerals that may also be exploited, including heavy metal minerals with potential environmental contamination risks [2].

Geologically, Kluet Tengah District is located within the Kluet Fault complex and is part of the Tapaktuan Volcanic Formation (Muvt). This formation consists of volcanic and pyroclastic rocks such as basalt, andesite, breccia, tuff, agglomerate, as well as sedimentary rocks and alteration

minerals formed through magmatic and hydrothermal activities [1]. These geological conditions suggest that the area has undergone complex mineralization processes, including iron mineralization that may be associated with copper and other sulfide minerals.

Previous studies in the Menggamat area, Kluet Tengah District, indicate that the iron ore deposits are dominated by hematite with relatively high Fe_2O_3 content. X-Ray Diffraction (XRD) and X-Ray Fluorescence (XRF) analyses revealed that hematite is the primary mineral phase, with Fe_2O_3 content reaching 85.31%, accompanied by silicate minerals as gangue [3]. Nevertheless, these studies remain preliminary and lack detailed mineragraphic analyses capable of explaining mineral textures, mineral associations, and the paragenetic sequence at the microscopic scale.

Mineralogical studies of iron ore deposits in other regions of Indonesia show that iron ores commonly consist of several economic minerals such as magnetite, hematite, goethite, and siderite, along with associated minerals including pyrite, quartz, and various oxide minerals [6], [7]. The presence of associated minerals, particularly sulfide minerals, is critical to assess due to their potential to generate acid mine drainage when exposed to oxygen and water. Therefore, identifying both main ore minerals and associated minerals is a crucial initial step in mitigating environmental impacts related to mining activities.

Mineragraphy is an effective method for identifying ore and associated minerals based on their optical properties, textures, and inter-mineral relationships. This method provides essential information on ore textures such as intergrowth, replacement, open space filling, and inclusion, which are closely related to the genesis of ore deposits [6]. Meanwhile, X-Ray Diffraction (XRD) analysis is used to accurately identify mineral phases, including those that are difficult to distinguish optically. The combined application of mineragraphic analysis and XRD has been widely employed in iron ore mineralogical studies and has proven to yield comprehensive results [3], [6].

Based on these considerations, this study is directed toward identifying the main ore minerals and associated minerals within iron ore deposits in Kluet Tengah District, particularly in Simpang Tiga villages, using an integrated mineralogical approach. This research also aims to examine microscopic textural characteristics and interpret the genetic tendencies of the iron ore deposits based on mineragraphic and XRD analyses. The results are expected to provide essential baseline scientific data to support sustainable mineral resource management and to serve as a preliminary basis for evaluating potential environmental impacts of mining activities.

The novelty of this study lies in its integrated mineralogical investigation of iron ore deposits in Simpang Tiga areas, which have not been extensively reported in the scientific literature. Furthermore, this study emphasizes the identification of associated minerals with potential environmental implications, thereby contributing not only to the advancement of geoscientific knowledge but also offering practical benefits for communities and stakeholders involved in mining management in South Aceh.

II. The Proposed Method

The proposed method applies a systematic and integrated mineralogical approach to characterize iron ore deposits in Kluet Tengah District, South Aceh, Indonesia. The workflow is designed in sequential stages to ensure data traceability, analytical reproducibility, and consistency of interpretation.

A. Field Data Acquisition

Field investigations were conducted at iron ore occurrences in Simpang Tiga villages. Geological observations focused on lithology, structural features, alteration characteristics, and mineralization styles. Rock samples were collected using channel sampling, chip sampling, and grab sampling to represent variations in lithology and mineralized zones. A total of 31 samples were collected from seven sampling locations. Each sampling point was documented with geographic coordinates, outcrop conditions, and photographic records.

B. Pre-Processing and Macroscopic Analysis

All samples were cleaned, labeled, and subjected to macroscopic analysis. Observations included color, texture, grain size, hardness, magnetic properties, and reaction with dilute HCl to

identify carbonate minerals. The results of this stage were used to select representative samples for subsequent laboratory analyses.

C. Sample Preparation

Selected samples were prepared as thin sections for petrographic analysis and polished sections for mineragraphic analysis. Sample preparation followed standard mineralogical laboratory procedures to ensure analytical accuracy and repeatability.

D. Mineragraphic Analysis

Mineragraphic analysis was performed using reflected-light microscopy to identify ore minerals and associated minerals based on their optical properties and textural relationships. Observed parameters included mineral type, relative abundance, and ore textures such as replacement, intergrowth, inclusion, open space filling, and crosscutting relationships. These textural features were used to interpret the paragenetic sequence and multistage mineralization processes.

F. Data Integration and Interpretation

Field observations, macroscopic descriptions, and mineragraphic results were integrated and comprehensively interpreted. This integrated dataset was used to identify the main ore minerals, associated minerals, microscopic textural characteristics, and the genetic tendencies of the iron ore deposits. The structured methodological framework enhances the reliability of mineralogical interpretations and supports environmental assessment and resource evaluation.

III. Method

This study applies a systematic mineralogical approach to characterize iron ore deposits in Kluet Tengah District, South Aceh. The methodology consists of field surveys, macroscopic analysis, microscopic analysis (petrography and mineragraphy), and integrated data interpretation to ensure consistency and reproducibility of the results.

A. Study Area

The study area is located in Simpang Dua and Simpang Tiga villages, Kluet Tengah District, South Aceh Regency, Indonesia. Geologically, the area lies within the Kluet Fault complex and is associated with the Tapaktuan Volcanic Formation, which is composed of volcanic, pyroclastic, and sedimentary rocks that have undergone alteration. with details summarized in Table I.

Table 1. Sampling Locations and Methods

No	Location (Coordinates)	Sampling Method	Rock Type	Number of Samples
1	N 03°11′04″, E 097°20′042″	Rock sampling	Sedimentary	1
2	N 03°11′899″, E 097°19′297″	Soil sampling	Sedimentary	1
3	N 03°12′028″, E 097°19′161″	Channel sampling (15 m)	Igneous and Metamorphic	8
4	N 03°12′030″, E 097°19′156″	Chip sampling	Metamorphic	3
5	N 03°11′939″, E 097°19′303″	Channel sampling (15 m)	Metamorphic	3
6	N 03°11′903″, E 097°19′197″	Channel sampling (15 m)	Metamorphic	5
7	N 03°12′041″, E 097°19′173″	Channel sampling (15 m)	Metamorphic	25

B. Field Survey and Sampling

Field surveys were conducted to document lithology, geological structures, alteration characteristics, and mineralization indications. Rock samples were collected from iron ore–bearing outcrops using channel sampling, chip sampling, and grab sampling methods. A total of 31 rock samples were collected from seven sampling locations. Each sampling site was recorded with geographic coordinates and photographic documentation.

C. Macroscopic Analysis

All samples were subjected to macroscopic analysis to identify the physical characteristics of the rocks, including color, texture, grain size, hardness, magnetic properties, and their response to dilute HCl solution as an indicator of the presence of carbonate minerals. This stage was intended to obtain preliminary mineralogical information and served as the basis for selecting representative samples for subsequent microscopic analysis. Macroscopic observations were conducted on all rock samples by examining their physical properties, as shown in Figure 1.

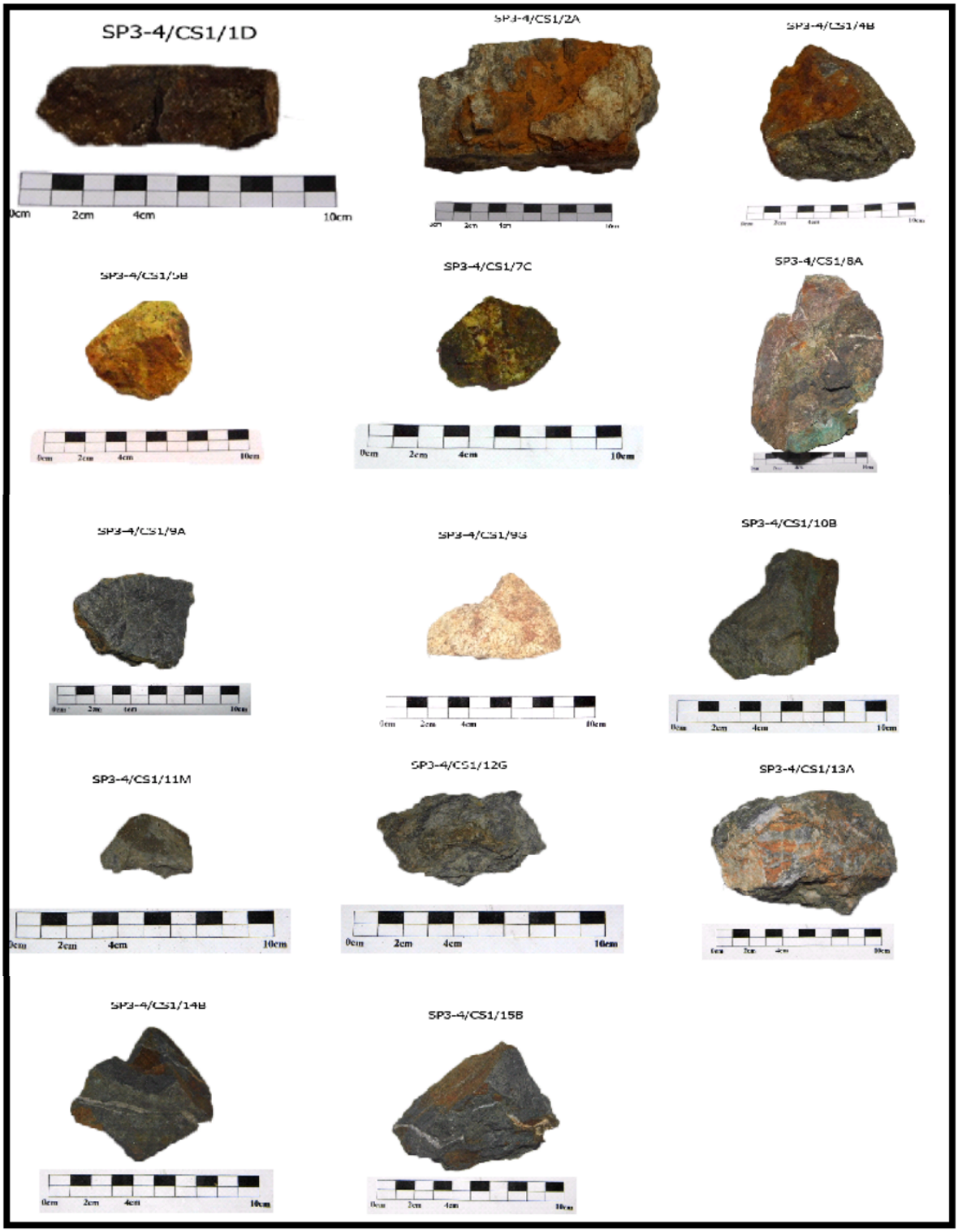

Fig 1. Macroscopic observation of rock samples

D. Sample Preparation

Selected samples were systematically prepared as thin sections for petrographic analysis and polished sections for mineragraphic analysis. The preparation process included initial cutting of the rock samples, mounting on glass slides, grinding, fine polishing, and thickness control to meet standard microscopic observation requirements. All preparation stages were conducted in accordance with established mineralogical laboratory procedures (Figures 2–5) to ensure optimal section quality, minimize preparation-induced errors, and guarantee the reliability and accuracy of subsequent microscopic analyses.

Fig 2. Polished Section from Channel Sampling 1

Fig 3. Polished Section from Channel Sampling 2

Fig 4. Polished Section from Location 5

Fig 5. Polished Section from Channel Sampling 3

E. Petrographic and Mineragraphic Analyses

Ore microscopic analysis was conducted on rock samples collected from the study area following the preparation stage, which involved the production of polished sections for mineragraphic analysis and thin sections for petrographic analysis. The selection of samples for polished section preparation was based on textural characteristics and the inferred abundance of ore minerals. The selected samples were subsequently prepared as polished and thin sections.

Microscopic observations were carried out using a ZEISS AXIO Imager A2m reflected–transmitted light polarizing microscope for polished sections and a Nikon Eclipse LV100POL microscope for thin sections. Mineragraphic investigations utilizing reflected-light polarization were performed using the Nikon Eclipse LV100POL microscope. Photomicrographs of the identified minerals were obtained using the same microscope equipped with a Nikon DXM1200C camera (Figure 3). To support the imaging process, NIS Elements 2.30 and Axio Vision LE software were employed with specific settings adjusted to meet the analytical requirements.

(a) (b)

Fig 3. Ore Microscopic Analysis Equipment: (a) Zeiss AXIO Imager A2m and (b) Nikon Eclipse LV100POL

F. Data Integration and Interpretation

Field observations, macroscopic descriptions, petrographic data, and mineragraphic results were integrated and comprehensively interpreted to identify the main ore minerals, associated minerals, microscopic textural characteristics, and the genetic tendency of the iron ore deposits.

IV. Results and Discussion

a. Results of Macroscopic Analysis

Based on the macroscopic observation data presented in Table 2, variations in lithology, physical properties, and chemical responses indicate significant heterogeneity of the rock units, reflecting differences in geological processes and the intensity of alteration and mineralization along the channel sampling lines. In general, uniform lithologies dominate at meters 1, 3, 6–8, and 12–15, characterized by massive textures, gray to dark coloration, relatively high hardness (>5 on the Mohs scale), and predominantly positive HCl reactions, suggesting a significant carbonate mineral content. In contrast, variable lithologies observed at meters 2, 4, 5, and 9–11 exhibit pronounced differences among sub-samples in terms of color, hardness, and HCl reaction, indicating heterogeneous mineral compositions and localized alteration intensity.

Table 2. Channel Sampling Data

Meter	Lithology (Uniform/Variable)	Number of Samples	Magnetic Response	HCl Reaction	Hardness (Mohs)	Color (Macroscopic)	Texture
1	Uniform	5 (A–E)	No	No	<5	Dark gray–greenish	Massive
2	Variable	4 (A–D)					
	=	(B–D)	No	No	<5	Brownish	Massive
	≠	(A)	No	Yes	<5	Yellowish white	Massive
3	Uniform	2 (A–B)	No	Yes	<5	Yellowish white	Massive

Meter	Lithology (Uniform/Variable)	Number of Samples	Magnetic Response	HCl Reaction	Hardness (Mohs)	Color (Macroscopic)	Texture
4	Variable	9 (A–I)					
	≠	(A, B, I)	No	No	<5	Silvery, mixed with white quartz	Weathered
	=	(C, F, E, G)	No	Yes		Yellowish white	Massive
5	Variable	12 (A–L)					
	=	(D, E, G, H ,I,K,L,F)	No	Yes	<5	Yellowish white	Massive
	≠	(A, B, C)	No	No	>3	Yellowish white; quartz vein; pyrite	Slightly weathered
6	Uniform	1 (A)	No	Yes	>5	White to slightly gray	Massive
7	Uniform	13 (A–M)	No	No	>5	Dark gray to blackish	Massive
8	Uniform	9 (A–I)	Partial	Partial	>5	Brown, reddish black	Massive
9	Variable	19 (A–S)					
	=	(A–R)	No	Dominant	>5	Bluish dark gray	Massive
	≠	(S)	No	No		Yellowish white	Slightly weathered
10	Variable	17 (A–Q)				>5	
	=	(A,D–Q)	No	Dominant		Bluish dark gray	Massive
	≠	(B, C)	No	Partial		Quartz vein with pyrite and chalcopyrite	Slightly weathered
11	Variable	16 (A–P)					
	=	(A–P except M)	No	Yes	>5	Brown oxidized exterior, gray interior, white spots	Massive
	≠	(M)	No	No	7	Vuggy quartz	Porous
12	Uniform	12 (A–L)	No	Yes	8	Dark gray	Massive
13	Uniform	5 (A–E)	No	Yes	6	Gray mixed with black, quartz veins	Massive
14	Uniform	9 (A–I)	No	Yes	6	Dark bluish gray, carbonate veins, iron oxidation	Massive
15	Uniform	5 (A–E)	No	Yes	6	Bluish gray, carbonate veins, iron oxidation	Massive

Magnetic responses were generally absent across most samples, with the exception of meter 8, which exhibited partial magnetic behavior, implying the limited presence of ferromagnetic minerals. Dominant HCl reactions recorded in several variable intervals (e.g., meters 9–11) support the interpretation of carbonate-rich zones, likely associated with skarn-type alteration. The occurrence of quartz veins accompanied by sulfide minerals such as pyrite and chalcopyrite, particularly at meters 5, 10, and 11, reflects hydrothermal fluid activity and is potentially directly related to metallic mineralization zones. Furthermore, slightly weathered to porous textures observed in certain sub-samples indicate localized supergene weathering processes. Overall, the macroscopic characteristics suggest strong lithological and structural controls on the distribution of alteration and mineralization within the study are

b. Results of Mineragraphic Analysis

In the photomicrograph SP3-4/CS1/1A (Fig 6), quartz minerals appear dark gray under plane-polarized light and transparent white under crossed polars. Within the quartz, pyrite minerals are observed with a bright gray color and isotropic characteristics, and they have undergone a replacement process, as indicated by their anhedral shapes and the presence of remnant island-like cavities representing former spaces occupied by pyrite minerals.

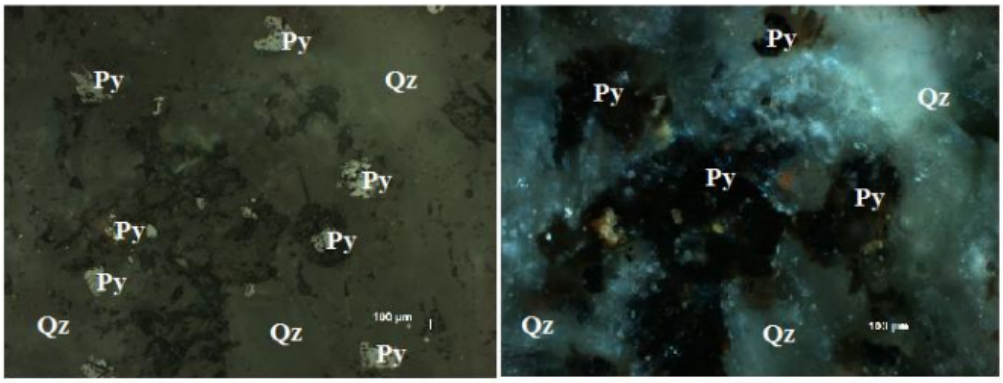

Fig 6. Photomicrograph of SP3-4/CS1/1A

Paragenetically, pyrite formed contemporaneously with quartz minerals, followed by a subsequent stage in which quartz began to replace the pyrite, as evidenced by the development of replacement textures. In Fig 7, the photomicrograph of the section coded SP3-4/CS1/5F shows the presence of quartz veins hosting pyrite and chalcopyrite mineralization. These minerals exhibit partial replacement textures by quartz, as well as inclusion textures in which chalcopyrite grains are entrapped within the quartz mineral.

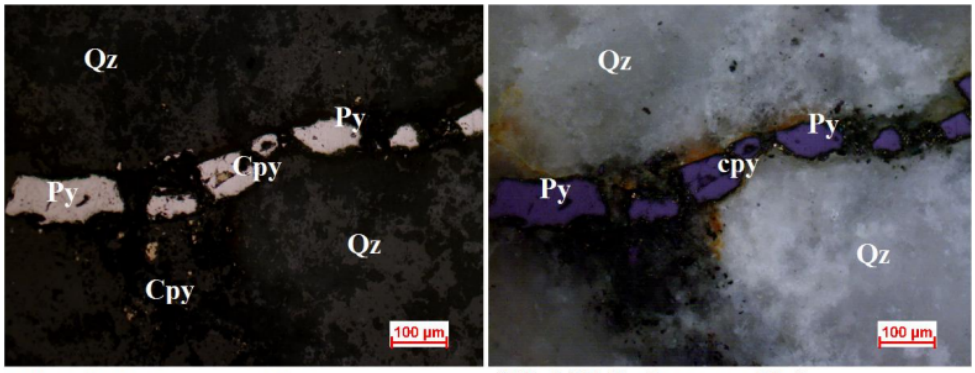

Fig 7. Photomicrograph of SP3-4/CS1/5

Based on the paragenetic sequence, quartz formed contemporaneously with pyrite and chalcopyrite. At a subsequent stage, pyrite and chalcopyrite underwent replacement processes, as indicated by portions of the volumes of both minerals being replaced by quartz.

The photomicrograph of the polished section SP3-4/CS1/12C (Fig 8) shows anhedral, dull yellow chalcopyrite occurring between quartz grains and exhibiting intergrowth textures with pyrite. The pyrite displays subhedral to anhedral habits and evidence of deformation. Replacement textures are evident, with quartz partially replacing pyrite and, to a lesser extent, chalcopyrite.

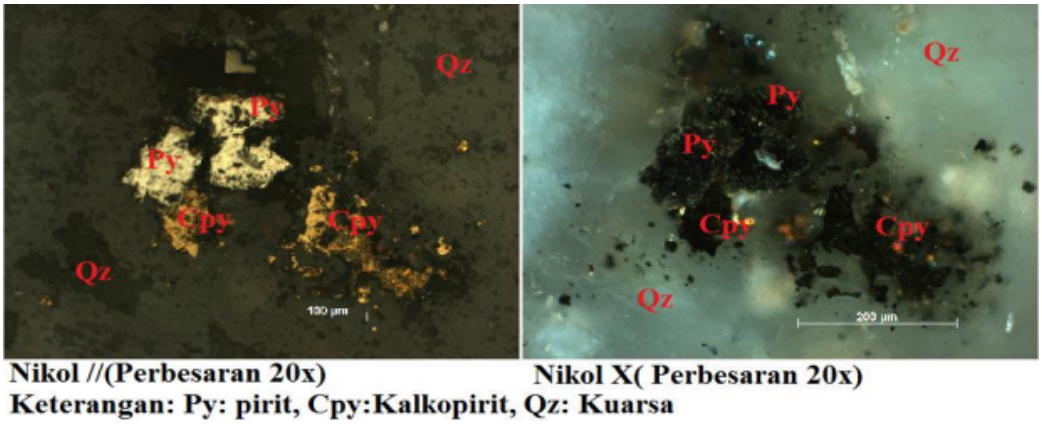

Fig 8. Photomicrograph of SP3-4/CS1/12C

Based on these textural relationships, pyrite and chalcopyrite are interpreted as early-formed mineral phases. Subsequently, quartz precipitated at a later stage and progressively replaced both sulfide minerals during ongoing alteration processes.

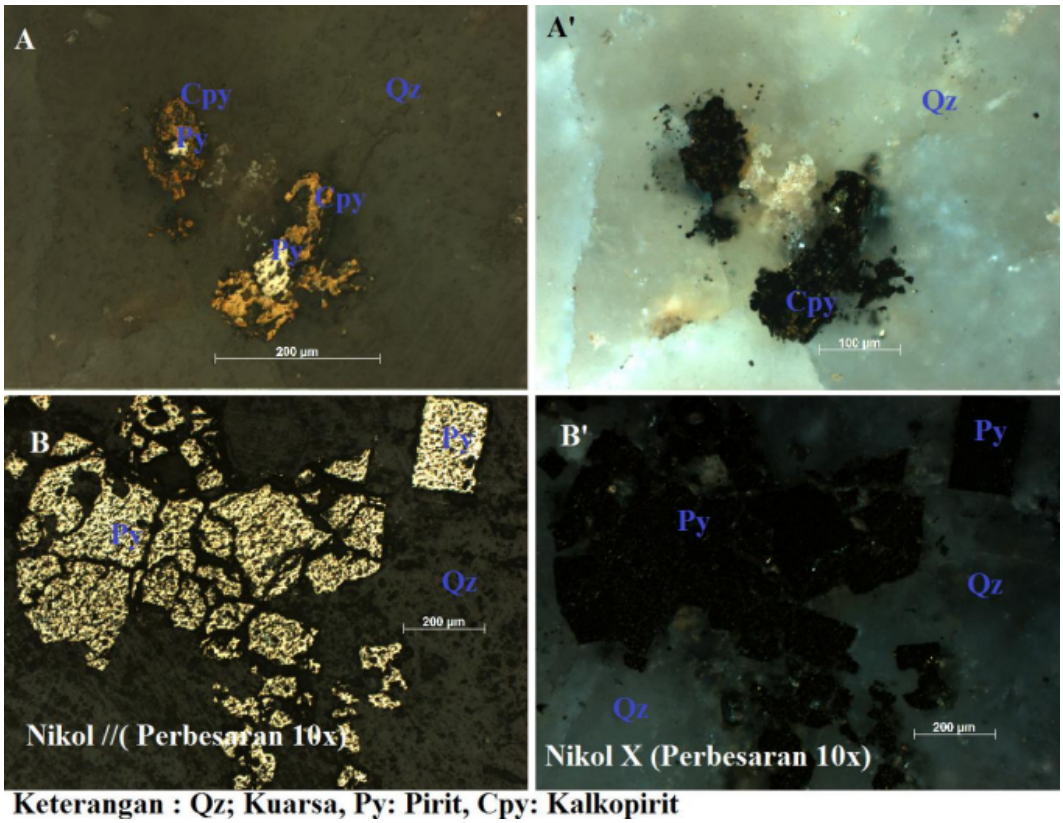

Fig 9. Photomicrograph of SP3-7/CS2/5A

In Figure 9, the photomicrograph of the polished section SP3-7/CS2/5A on section A–A′ shows chalcopyrite with a dull reddish-yellow color and an anhedral form, mineralized within quartz and enclosing pyrite inclusions. On section B–B′, pyrite occurs with euhedral to anhedral habits, partially deformed, and is progressively replaced by quartz. The paragenetic interpretation for section A–A′ indicates that pyrite and chalcopyrite formed at an early stage and were subsequently partially replaced by quartz. In section B–B′, the quartz replacement of pyrite is more pronounced, confirming that quartz represents a later-stage mineral phase.

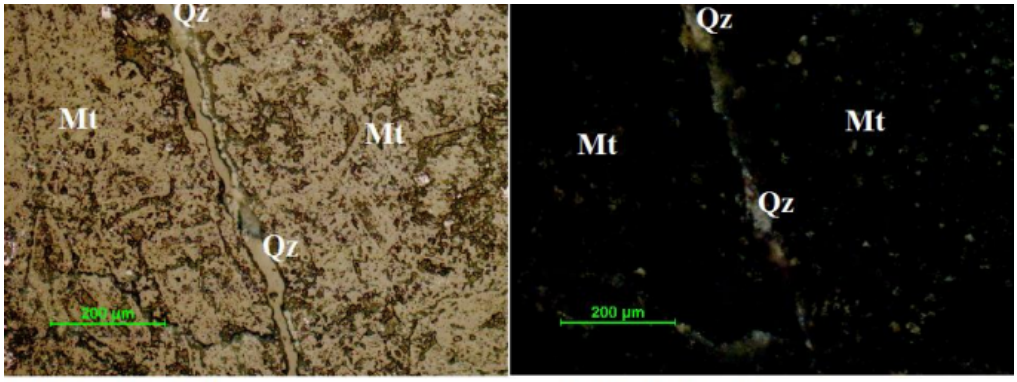

Fig 10. Photomicrograph of SP3-8/CS3/1A

Figure 10 shows the photomicrograph of the polished section coded SP3-8/CS3/1A, which displays a distinct crosscutting texture, indicated by magnetite being cut by a quartz vein. This condition suggests that magnetite formed at an earlier stage, followed by quartz precipitation during a subsequent mineralization phase. The quartz vein that crosscuts the magnetite exhibits a clear cutting relationship, texturally confirming that quartz represents a younger mineral phase that filled fractures or openings formed after the crystallization of magnetite. This relationship also reflects the involvement of hydrothermal fluids transporting silica and depositing it as quartz, thereby crosscutting and partially replacing the pre-existing magnetite mineral.

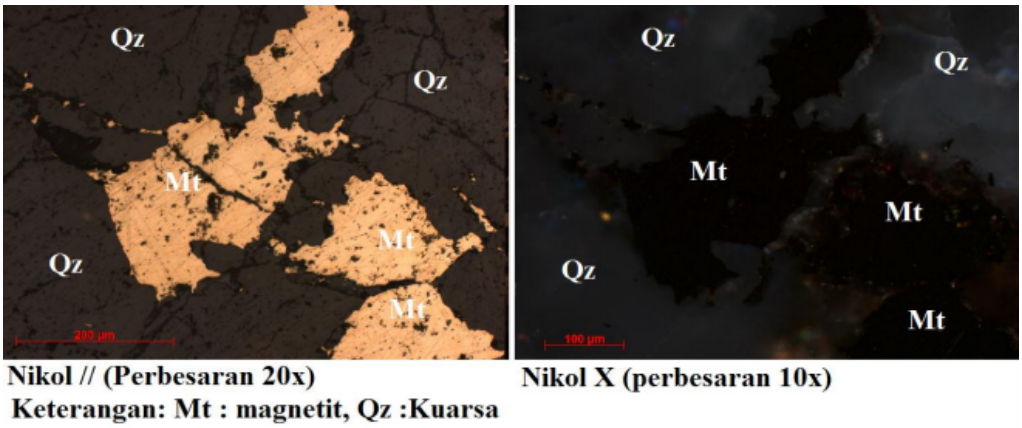

Fig 11. Photomicrograph of SP3-8/CS3/4A

The photomicrograph of the polished section SP3-8/CS3/4A (Figure 11) shows a replacement texture between magnetite and quartz. Magnetite appears brownish cream in color with predominantly concave grain boundaries, indicating that the mineral has undergone partial dissolution. In contrast, the replacing quartz exhibits convex grain boundaries, representing the growth of a new mineral phase that occupies the space formerly filled by magnetite.

This concave–convex boundary texture is a characteristic feature of replacement processes, reflecting the textural relationship between the replaced and replacing minerals. Paragenetically, this condition indicates that magnetite formed at an earlier stage and was subsequently dissolved and progressively replaced by quartz during a later mineralization stage, likely associated with silica-rich hydrothermal fluid activity.

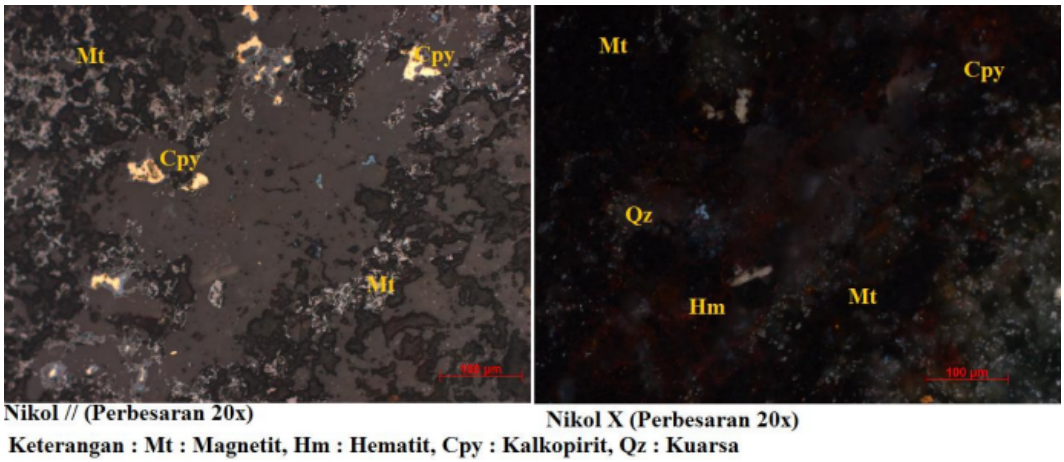

Figure 12. Photomicrograph of SP3-8/CS3/7A

Figure 12 shows the photomicrograph of the polished section SP3-8/CS3/7A, characterized by quartz veins crosscutting early-formed magnetite and carrying dull yellow chalcopyrite. Magnetite exhibits concave grain boundaries forming island-like remnants, indicating intensive replacement. Quartz partially replaces magnetite, followed by the formation of hematite that replaces magnetite and locally affects quartz and chalcopyrite.

The photomicrograph in Figure 13 shows a replacement texture between magnetite and garnet. Magnetite displays concave grain boundaries due to partial dissolution, whereas garnet shows convex boundaries, indicating growth as a replacing mineral. These textures confirm a paragenetic sequence in which magnetite formed first and was subsequently replaced by quartz, hematite, and garnet during later hydrothermal alteration stages.

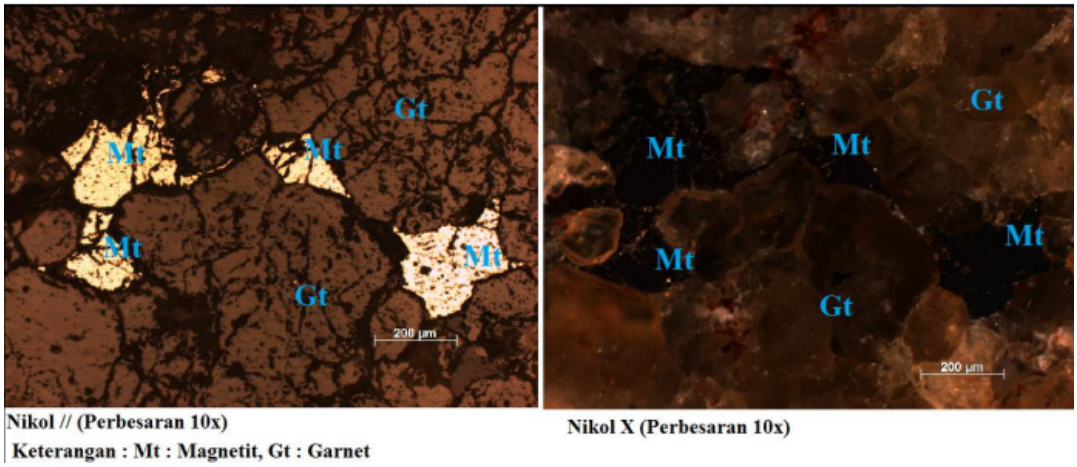

Fig 13. Photomicrograph of SP3-8/CS3/12A

In the photomicrograph SP3-8/CS3/12A, the paragenetic sequence indicates that magnetite represents an early-formed mineral phase that was subsequently and progressively replaced by garnet. This replacement likely resulted from metamorphic or hydrothermal fluid activity enriched

in Ca, Fe, and Al. The process reflects changes in the physicochemical conditions of mineral formation, such as increased fluid activity, variations in pressure–temperature conditions, or changes in fluid chemistry, which facilitated garnet crystallization and the replacement of magnetite.

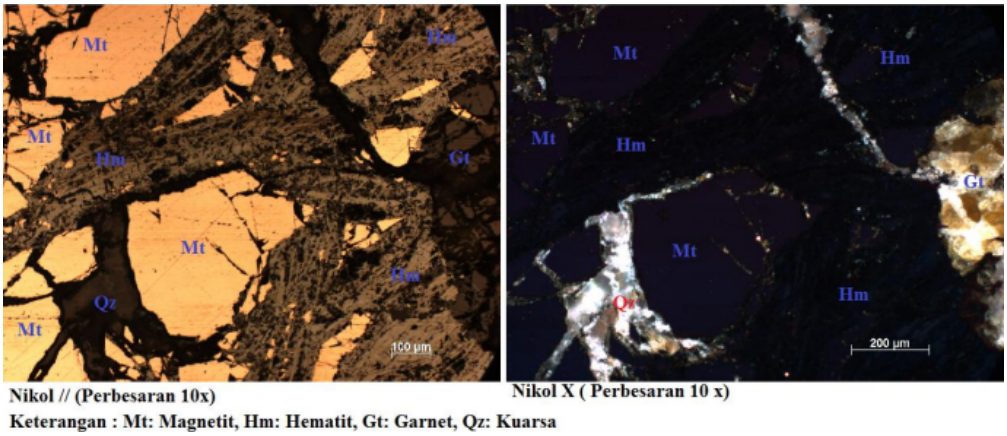

Fig 14. Photomicrograph of SP3-8/CS3/16A

Figure 14 shows a polished-section photomicrograph of SP3-8/CS3/16A characterized by replacement and crosscutting textures. Magnetite, initially massive, was deformed and fractured, followed by partial dissolution and replacement by bluish-gray hematite, indicating oxidation under hydrothermal or low-grade metamorphic conditions. Garnet locally replaces magnetite along grain boundaries, suggesting a later formation stage related to changing pressure–temperature conditions or fluid chemistry. Quartz veins crosscut magnetite, hematite, and garnet, confirming quartz as the youngest mineral phase, precipitated from late-stage silica-rich fluids.

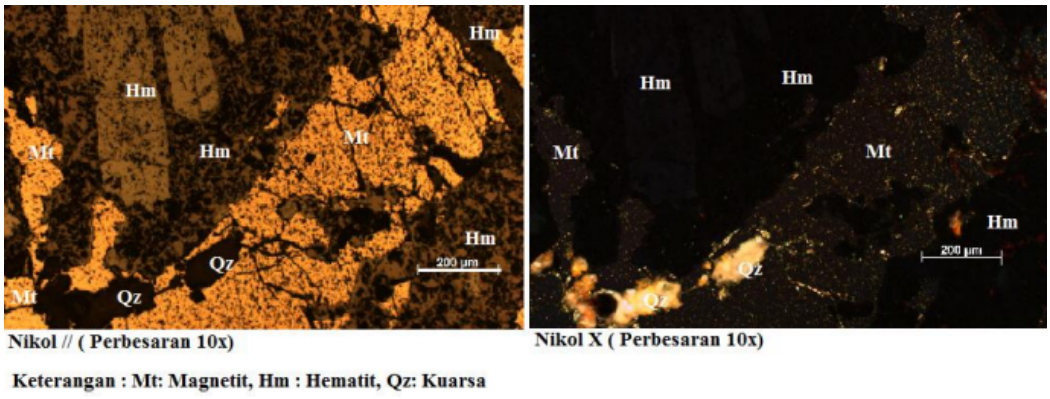

Fig 15. Photomicrograph of SP3-8/CS3/19E

Figure 15 shows a replacement texture in which cream-colored, isotropic magnetite is partially replaced by brownish-gray hematite, indicating oxidative alteration by mineralizing fluids. Magnetite represents an early mineral phase, whereas hematite is a younger replacement phase. The process initiates along grain boundaries and fractures, producing concave boundaries on magnetite and convex growth boundaries on hematite, with remnant magnetite preserved as isolated islands within the hematite matrix.

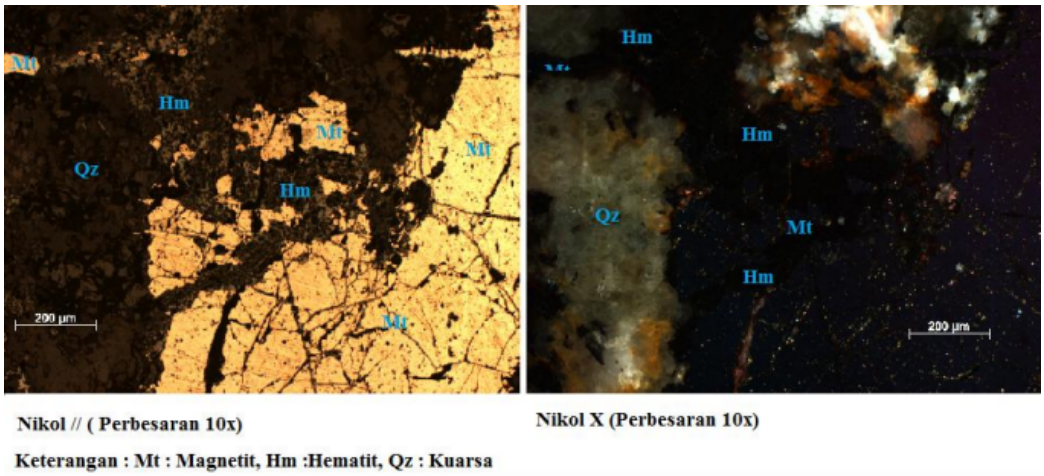

Fig 16. Photomicrograph of SP3-8/CS3/20A

The polished-section photomicrograph in Figure 16 displays a replacement texture in which cream-colored, isotropic magnetite is progressively replaced by bluish gray hematite. This replacement occurs through chemical reactions between magnetite and mineralizing fluids, advancing from grain boundaries and fractures toward the crystal interiors. Texturally, magnetite shows concave dissolution boundaries, whereas hematite exhibits convex growth boundaries, with remnant magnetite preserved as isolated islands. These features indicate that magnetite formed earlier and was subsequently replaced by hematite during oxidative alteration.

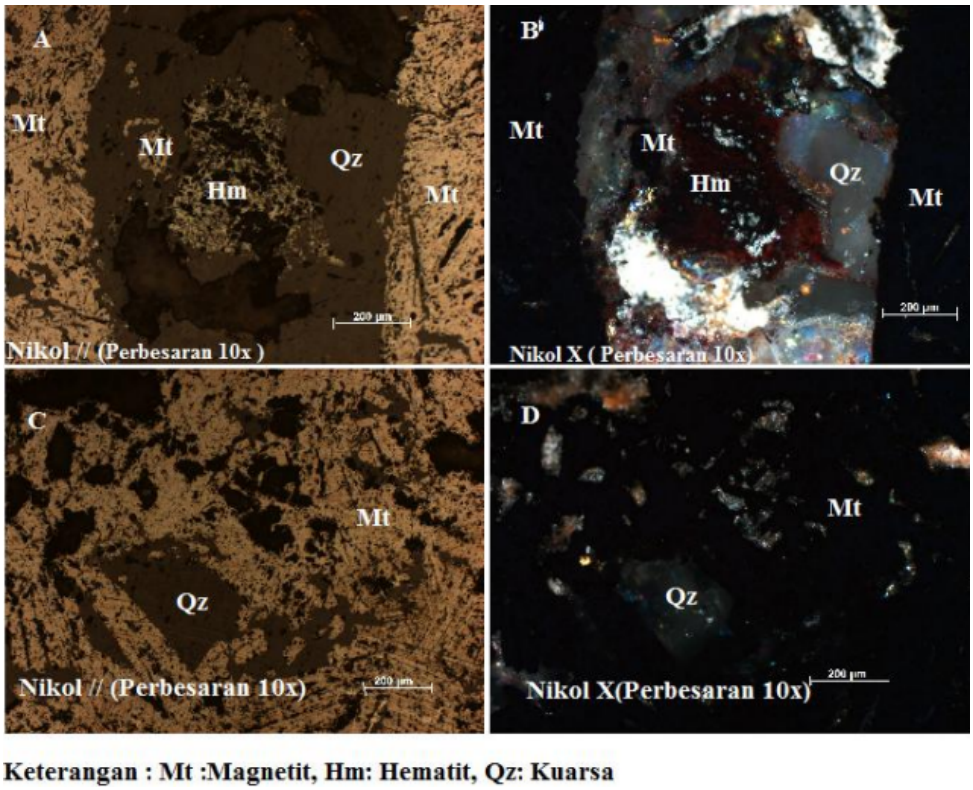

Fig17. Photomicrograph of SP3-8/CS3/23E

Figure 17 illustrates a crosscutting relationship that is critical for paragenetic interpretation. In sections A–B, dark gray quartz veins crosscut cream-colored, isotropic magnetite and carry hematite showing red internal reflections, confirming that quartz is a younger mineral phase. In sections C–

D, magnetite remains isotropic, while quartz appears anisotropic, further supporting the interpretation that quartz postdates magnetite and hematite unless subsequent replacement has occurred.

The photomicrograph observations provide comprehensive insight into the mineralogical characteristics, textural relationships, and paragenetic evolution of the mineralization in the study area. The identified ore minerals include magnetite, hematite, pyrite, and chalcopyrite, accompanied by gangue and alteration minerals such as quartz, garnet, and carbonate minerals. The diversity of textures replacement, crosscutting, intergrowth, inclusion, and oxidation indicates a multistage mineralization process controlled by evolving physicochemical conditions and hydrothermal fluid activity.

Magnetite is consistently observed as an early-formed mineral, commonly displaying massive textures and isotropic optical properties. Subsequent deformation and fracturing of magnetite facilitated fluid ingress, leading to partial dissolution and replacement by hematite, as evidenced by concave grain boundaries and remnant magnetite islands. This magnetite-to-hematite transformation reflects an oxidative alteration process, likely associated with increasing oxygen fugacity during later hydrothermal stages or low grade metamorphism.

Quartz plays a significant role as a late-stage mineral phase, as demonstrated by its pervasive crosscutting relationships with magnetite, hematite, pyrite, and chalcopyrite. Quartz veins frequently occupy fractures and voids, confirming precipitation from silica-rich hydrothermal fluids after the formation of earlier ore minerals. In several samples, quartz also exhibits replacement textures, partially substituting sulfide minerals such as pyrite and chalcopyrite, further emphasizing its role during the later stages of mineralization.

Sulfide minerals, particularly pyrite and chalcopyrite, generally represent early to intermediate mineralization phases. Their occurrence as inclusions within quartz and their partial replacement by quartz suggest synchronous formation followed by re-equilibration during subsequent fluid events. Intergrowth textures between pyrite and chalcopyrite indicate co-precipitation under similar physicochemical conditions, whereas later replacement by quartz reflects changing fluid chemistry and temperature.

The presence of garnet replacing magnetite provides strong evidence for contact metasomatism, consistent with skarn type mineralization. Garnet formation requires Ca, Fe, and Al-rich fluids, indicating interaction between intrusive magmatic bodies and carbonate host rocks. The concave convex boundary relationships between magnetite and garnet further support a metasomatic replacement mechanism rather than simple overgrowth.

Overall, the photomicrograph data reveal a clear paragenetic sequence: (1) early formation of magnetite and sulfide minerals (pyrite chalcopyrite), (2) oxidative alteration and partial replacement of magnetite by hematite, (3) metasomatic replacement by garnet, and (4) late-stage quartz veining and replacement driven by silica-rich hydrothermal fluids. These observations collectively support the interpretation of a skarn-type iron mineralization system that evolved through multiple hydrothermal and metasomatic events, strongly influenced by structural controls and fluid–rock interactions.

V. Conclusion

This study concludes that mineralization in the Menggamat area is characterized by the presence of primary ore minerals, namely magnetite and hematite, which indicate a high economic potential as iron ore resources with a primary deposit nature. In addition to the main iron ore minerals, associated metallic minerals such as chalcopyrite were identified, suggesting potential for copper mineral extraction. Non-ore minerals are dominated by calcite, which constitutes the primary component of

the limestone host rock. Another significant mineralogical finding is the occurrence of garnet, indicating the development of a contact metasomatic zone that is closely associated with the Kluet Fault system and plays an important role in controlling the mineralization processes in the study area.

Acknowledgment

This research was supported by the Directorate of Research and Community Service, Ministry of Higher Education, Science, and Technology, Indonesia (2025).

References

[1] Cameron.N.R,Bennet. J. D, Bridge. D. McC., Djunudin. A,Ghazali. S. A, Harahap, H. Geologi Lembar Tapaktuan, Sumatra. 1982. Departemen Pertambangan dan Energi Direktotat Jendral Pertambangan Umum Pusat Penelitian dan Pengembangan Geologi.

[2] Syarifah. R, Tasbi. H. Penyalahgunaan Pengelolaan Pertambangan Terhadap Kerusakan Lingkungan Hidup di Kecamatan Kluet Tengah. Legitimasi. 2018:7(1):149-171

[3] Adi.R, Zulkarnain.J Kajian Awal Karakteristik Mineral Magnetik Bijih Besi Menggamat, Aceh Selatan In: Prosiding Seminar FMIPA Universitas Lampung. 2013.p:203-206

[4] Lindawati,Mursal, Identifikasi Mineral Pada Batu marmer dari gunung Kerambil Aceh Selatan Menggunakan Difraksi Sinar-X.J.Aceh Phys.2018:7(3):p:152-156

[5] Analiser,H. Eksplorasi Pendahuluan untuk menentukan penyebaran bijih besi sebagai sebagai mineral ikutan di daerah Penuntungan Kecamatan Penanggalan dan Sekitarnya , Kota Subulussalam ,Provinsi Aceh.Jurnal Sain dan Teknologi ISTP.2021:15(1):p51-63

[6] Thamsi,A.B, Bakri.H, Harwan, Nasrullah, Aswadi.M, Karakteristik Mineralogi Bijih Besi Daerah kadong Kadong, Kabupaten Luwu,Provinsi Sulawesi Selatan.Jurnal Pertambangan.2021:5(4):p.158-16

[7] Rian Adriansyah, Model Genesa Endapan Besi di Kecamatan Kendawang, Ketapang, Kalimantan Barat. JAPPS.2019:1(2): p41-46]